Macromolecules
ARTICLE

Macromolecules **2010**, *43*, 7277–7281 **7277**
DOI: 10.1021/ma101231z

Microgels with an Interpenetrating Network Structure as a Model System for Cell Studies

Neta Raz, James K. Li, Lindsey K. Fiddes, Ethan Tumarkin, Gilbert C. Walker, and Eugenia Kumacheva*

Department of Chemistry, University of Toronto, 80 Saint George Street, Toronto, Ontario M5S 3H6, Canada

Received June 2, 2010; Revised Manuscript Received July 19, 2010

ABSTRACT: This paper reports the preparation of microgels with an interpenetrating polymer network (IPN) structure using microfluidic synthesis. Microgels with a narrow size distribution were generated from ionically cross-linked alginate and chemically cross-linked poly(*N*-isopropylacrylamide). The mechanical properties of the microgels, such as Young's modulus and the characteristic relaxation time, were studied using atomic force microscopy (AFM). The lower limits of the elasticity found in this study are within the range of the elasticity reported for neutrophils, making these microgels a promising model system for studies of cell flow through constrained geometries.

Introduction

Studies of the flow of blood cells in the cardiovascular system have great importance for understanding the function of the cells and finding cure to diseases related to blood flow, e.g., atherosclerosis. In particular, studies of flow of neutrophils in the pulmonary capillary network have generated much attention. Since the average diameter of neutrophils of 6−9 μm is up to 40% larger than the diameter of lung capillary segments,[1] neutrophils should undergo substantial deformation in order to traverse a capillary. In addition, white blood cells are significantly more rigid than red blood cells,[2] and in comparison with erythrocytes that flow through the lung microcirculation within several seconds, the flow of neutrophils can take more than 20 min.[1] This delay causes an increase in the concentration of neutrophils in the lungs and an increase in pressure at the capillary segment entrance.[1] The delay may lead to the leukocyte plugging phenomenon, caused by adherence of the cells to the endothelium and hinder to the flow of blood.[2,3] These effects motivated studies of the relation between the mechanical properties of neutrophils and their deformation and flow under confinement.

The mechanical properties of neutrophils have been studied by various techniques. The value of Young's modulus of passive neutrophils reported in the literature ranged from 200 to 2800 Pa.[4,5] Under stimulation, neutrophils may become stiffer or softer. For example, it was found that while the Young's modulus of resting lymphocytes hybridoma was 1.4 kPa, the modulus of treated cells decreased to 0.30 kPa or increased up to 3.0 kPa, depending on the stimulus.[6] Protrusional stiffness of the surface of human neutrophils measurements using an optical trap varied from 0.06 to 0.11 pN/nm.[8] Neutrophils' stiffness did not change upon heating from room temperature to 37 °C, and the viscoelastic behavior of the cells was proven in relaxation time experiments. Micropipet aspiration was also widely used to study viscoelasticity and stress relaxation of human neutrophils.[2,9−11] The viscosity of neutrophils, studied mainly by micropipet aspiration, was in the range from 6.5 to 89 Pa·s, depending on the model chosen to describe the cells.[12] Yanai et al.[13] found that stress relaxation of neutrophils showed power law behavior as a function of time with an exponent of ∼0.5.

Studies of flow of cells are challenging for a number of reasons. For example, understanding the role of specific factors on cell behavior is difficult due to the large variability between cells. In addition, an accurate variation of a particular single variable, e.g., the value of elastic modulus or the adhesion of cells to the substrate, is sometimes impossible. Therefore, studies conducted on model systems—"surrogate" cells—are sometimes preferred.[14,15] The use of vesicles,[15,16] microgels[17,18] or gels encapsulated in vesicles[16,19,20] allowed control and consistent variation of their size and surface and mechanical properties.

Here we report on a microfluidic (MF) synthesis of "surrogate cells" based on polymer microgels with a double-network structure.[21,22] The microgels contained alginate cross-linked with Ca^{2+} ions (the first network) and poly(*N*-isopropylacrylamide) (the second network). We assumed that the formation of an interpenetrating polymer network (IPN) derived from the physically and chemically cross-linked polymers would enable the elasticity and relaxation time of the microgel to be controlled independently, whereas the MF synthesis would provide precise control of the microgel size and structure.[24−27] In the present work, the mechanical properties of the microgels were controlled by varying the concentration ratio between the polymers and the degree of cross-linking of poly(*N*-isopropylacrylamide) (PNIPAm). We note that the proposed approach to microgels with IPN structures is distinct from our previous work in which we produced rigid microbeads from the mixture of chemically cross-linked poly(tripropylene glycol diacrylate) and polyurethane by carrying two consecutive reactions.[23]

Experimental Section

Materials. $CaCl_2$ was purchased from Fisher Scientific (Canada). All other chemicals used in the present work were purchased from Sigma-Aldrich (Canada).

Composition of Microgels. The IPN microgels were prepared from sodium alginate which was physically cross-linked by Ca^{2+} ions and PNIPAm which was chemically cross-linked by *N*,*N*′-methylenebis(acrylamide) (BIS). The polymerization of *N*-isopropylacrylamide (NIPAm) monomer was initiated in redox reaction with the initiator ammonium persulfate (APS) and in the presence an accelerator *N*,*N*,*N*′*N*′-tetramethylethylenediamine (TEMED) at room temperature. The compositions

*To whom correspondence should be addressed.

Published on Web 08/11/2010

Table 1. Recipes Used for the Preparation of IPN Microgels

sample	content of sodium alginate[a] (wt %)	content of NIPAm[a] (wt %)	content of BIS[a,b] (wt %)	content of water[a] (wt %)	mean diameter of microgels (μm)
A1	1.0	1.0	10.0	97.8	103 ± 3
A2, B2, C2	1.0	4.0	10.0	94.5	89 ± 6
B1	1.0	4.0	1.0	94.9	99 ± 10
C1	0.5	4.0	10.0	95.0	138 ± 8.6
C3	1.5	4.0	10.0	93.0	98 ± 4.6
C4	2.0	4.0	10.0	93.5	103 ± 5.5

[a] Concentrations of reagents in the table are given for the droplet phase feed solutions. The continuous phase contained 0.25 wt % CaI_2, 1.0 wt % TEMED, and 2.0 wt % Span-80 in undecanol. [b] The concentration of BIS is given relative to the concentration of NIPAm.

of each of the microgel sample prepared are summarized in Table 1.

Characterization of Microgels. *Measurements of Microgel Dimensions*. The microgels were imaged using an optical microscope (Olympus BX51) equipped with a digital camera (CoolSnap ES, Photometrics, Roper Scientific). The diameters of at least 50 microgels were measured in each sample using ImagePro Plus 5 software (Media Cybernetics Inc.). The distributions of micorgel diameters were fitted to the Gaussian distribution.

Structure of Microgels. The internal structure of microgels was examined using confocal fluorescent microscopy. A fluorescent dye Fluo-3—a tracer for Ca^{2+} ions—was dissolved in the aqueous droplet phase and, upon emulsification, encapsulated in the droplets. Following gelation, the microgels were transferred to deionized (DI) water and imaged using a Leica TCS SP2 confocal microscope.

Swelling Ratio of Microgels. The swelling ratio of the microgels was measured for a macroscopic gel. Approximately 0.5 cm^3 of the solution with a composition given in Table 1 was prepared. A small Petri dish was filled with an aqueous solution of alginate, NIPAm, BIS, and APS to a height of about 5 mm. Subsequently, an undecanol solution with the same composition as the continuous phase in MF experiments was poured over the aqueous solution and left overnight for polymerization and cross-linking. After 24 h, the undecanol solution was replaced with the post-treatment aqueous solution for another 24 h. The resulting hydrogels were washed with deionized water and transferred to PBS buffer. Approximately 4 g of the sample was weighed in the swollen and dry states. The experiment was repeated three times for each sample. The swelling ratio was calculated as

$$Q = \frac{m_s}{m_d} \times 100 \tag{1}$$

where m_s and m_d are the masses of the swollen and dry hydrogel, respectively.

Mechanical Properties of Microgels. The Young's modulus of each microgel was determined in contact mode AFM indentation experiments, performed under fluid using an MFP-3D AFM (Asylum Research, Santa Barbara, CA) equipped with a 100 μm wide tipless cantilever (Nano World). The nominal spring constant value of the cantilever was ~0.03 N/m and more accurately determined by the thermal noise method.[28] To immobilize the microgels on the substrate and ensure that a microgel particle remains under the cantilever during the indentation measurement, the particles were applied to a gold-coated quartz substrate (Ssens B.V., Hengelo, The Netherlands) coated with a self-assembled monolayer of mercaptoethylamine.[29] The substrates were prepared by cleaning gold-coated quartz substrates with piranha solution rinsing them with excess deionized water, immersing them in a 1.0 mM mercaptoethylamine aqueous solution for at least 2 h, and finally washing them with an excess of DI water. The microgels that carried a negative charge due to the presence of deprotonated carboxylic groups in alginate were attracted to the positively charged substrate.

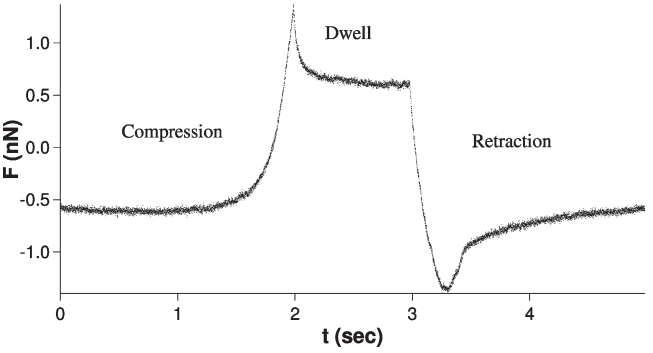

Figure 1. Typical force−time curve acquired for microgel particle obtained from sample C2 (see Table 1).

All AFM measurements were carried out in PBS buffer solution. For each microgel composition, we examined at least three microgel particles by collecting 10 force−distance curves for each of them. The force indentation results were fitted to the following equation using IgorPro software.[30]

$$\alpha = (3\pi)^{2/3} P^{2/3} \left(\frac{1-\sigma^2}{E}\right)^{2/3} \left(\frac{1}{D}\right)^{1/3} \tag{2}$$

where α is the indentation distance, P is the force (pN), σ is the Poisson's ratio (assumed to be 0.5), E is the Young's modulus (Pa), and D is the microgel diameter (μm).

The relaxation process of the microgels was studied in stress relaxation measurements. Figure 1 illustrates a typical force−time curve acquired in such experiments. First, a loading force was applied to compress a microgel particle until a set point of 1.5−2 nN was reached (the "compression" region). Then, the driving piezo was halted for 1−2 s (the "dwell" region), and during this time, a decay of the force, F, occurred, due to the relaxation of the stress on the microgel particle. After the dwell, the cantilever was retracted from the microgel (the "retraction" step).

The dwell portion of the force vs time curves was fitted to the Kohlrausch−Williams−Watts function (stretched exponential function) using IgorPro software.[31]

$$F(t) = F_r \exp\left[-\left(\frac{t}{\tau}\right)^{\beta}\right] + F_\infty \tag{3}$$

where F_r is the amplitude of the relaxation force (nN), F_∞ is the force after a length of time much longer than the mean relaxation time τ, and β is the stretching exponent. In cases where the system cannot be fitted to a single-exponential decay, the stretching exponent, β, gives a measure of the distribution of the relaxation times.

Experimental Design. The method for the preparation of microgels with the IPN structure included MF generation of droplets of the solution containing a mixture of sodium alginate (to generate the first network) and NIPAm and redox initiator (to form the second network), followed by the gelation of the precursor droplets. We followed a modified external gelation method reported elsewhere.[24,26] Figure 2 shows the schematic of the MF reactor, which consisted of a flow-focusing droplet generator[32] with an orifice width and height of 85 and 115 μm, respectively, and an extension serpentine channel with a length of 23.5 cm. The reactor was fabricated in poly(dimethylsiloxane) using a soft lithography method.[32] Two immiscible liquids—an aqueous droplet phase and undecanol continuous phase—were introduced in the central and side microchannels of the reactor, as shown in Figure 2. Undecanol contained 0.25 wt % CaI_2, 1.0 wt % TEMED, and 2.0 wt % surfactant Span-80. The aqueous phase contained 0.1 wt % APS and varying amounts of sodium

alginate, NIPAm, and BIS. The recipes used for the generation of microgels are shown in Table 1.

As the aqueous droplets moved in the downstream channel, Ca^{2+} ions and TEMED diffused from the continuous phase into the droplets, thereby causing gelation of alginate and polymerization and cross-linking of NIPAm[26,34] (Figure 2). The microgels collected at the outlet of the MF reactor were postgelled by transferring them into a solution of 2.0 wt % $CaCl_2$, 0.1 wt % APS, and 0.5 wt % TEMED in water for overnight incubation. After the postgeleation step, the microgels were washed with DI water and transferred to phosphate buffered saline (PBS, pH 7.4).

The effect of the composition of microgels on their mechanical properties was studied for three groups of microgels prepared using different formulations in three series of experiments (Table 1). In series A we varied the amount of NIPAm in the droplet phase from 1.0 to 4.0 wt %, while maintaining the concentrations of alginate and the cross-linking agent BIS constant. In series B the concentration of BIS in the droplet phase was increased from 1.0 to 10.0 wt % (the concentration of NIPAm and alginate were constant). In series C the concentration of sodium alginate in the droplet phase was varied from 0.5 to 2.0 wt % (the concentrations of NIPAm and BIS were constant).

Results and Discussion

In the present work, we produced microgels with the dimensions of $100 \pm 10\ \mu$m, convenient for AFM characterization and further optical microscopy imaging. The flow rate of the droplet phase was in the range from 0.05 to 0.1 mL/h; the flow rate of the continuous phase varied from 1.5 to 3.0 mL/h. Generally, a higher flow rate ratio of the droplet-to-continuous-phase was used for compositions of the droplet phase with higher viscosity.

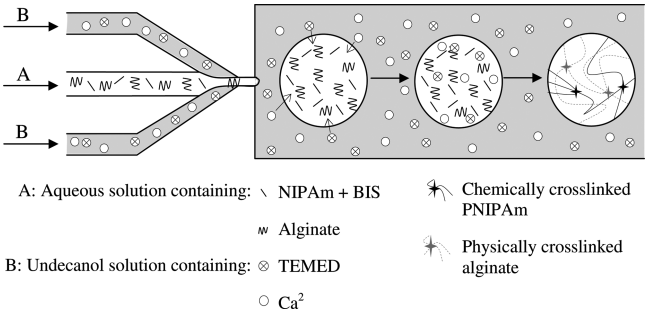

Figure 2. Schematic of the MF reactor for the synthesis of alginate−PNIPAm IPN microgels. TEMED and CaI_2 are dissolved in the continuous phase (undecanol), which is supplied to the MF reactor from streams B. Sodium alginate, NIPAm, BIS, and APS are dissolved in the aqueous droplet phase, which is introduced in the central channel (stream A). Following emulsification, TEMED and Ca^{2+} ions diffuse into the droplets and trigger polymerization of NIPAm and cross-linking of alginate, respectively.

Generation of microgels with smaller dimensions was possible by tuning the ratio of flow rates of the droplet and continuous phases.

Figure 3a shows a typical optical microscopy image of the microgel particles. The microgels were spherical and nearly transparent due to the high water content. Figure 3b represents a characteristic confocal microscopy image of the individual microgel particle stained with Fluo-3 dye. Since the fluorescence of the dye was enhanced in the presence of Ca^{2+} ions, a uniform distribution of fluorescence intensities throughout the particle suggests a homogeneous distribution of the cross-linked alginate in the microgel, with no significant macroscopic phase separation within the imaging resolution. The bright ring observed at the circumference of the microgel could be caused by the higher concentration of Ca^{2+} ions on the microgel surface as well as optical effects. After emulsification, precursor droplets showed a narrow size distribution and the relative standard deviation in the dimensions of the microgels following their postgelation, washing, and transfer into the buffer was in the range of 4.7−13%. Figure 3c shows a typical size distribution of the microgel particles.

We examined the effect of microgel composition, namely, the role of the concentration of alginate, PNIPAm, and the cross-linking agent on the swelling and the mechanical properties of the microgels. The effect of the sample composition on the swelling

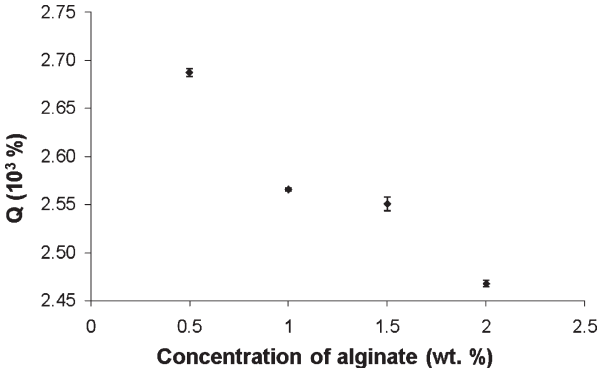

Figure 4. Effect of alginate concentration in the aqueous solution on the degree of swelling of the hydrogels. All aqueous solutions contained 4.0 wt % NIPAm and 10.0 wt % BIS (with respect to NIPAm).

Table 2. Swelling Ratio, Young's Modulus, and Relaxation Time of Microgel Particles Prepared from Samples A1, B1, A2, and B2

sample	swelling ratio, Q (10^3%)	Young's modulus, E (kPa)	relaxation time, τ (ms)
A1	7.28 ± 0.49	9.9 ± 1.6	64.2 ± 16.1
B1	3.46 ± 0.11	11.7 ± 1.4	46.3 ± 28.6
A2 and B2	2.57 ± 0.04	11.4 ± 2.0	69.1 ± 50.4

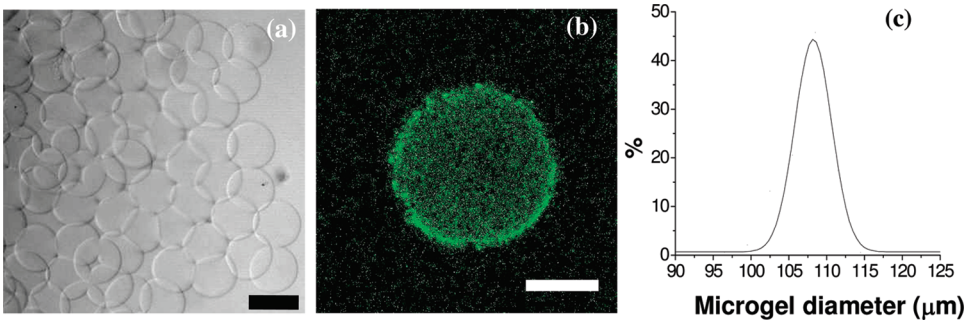

Figure 3. (a) Optical microscopy image of the microgels prepared from solution A1 (Table 1) and transferred to the PBS buffer. Scale bar 100 μm. (b) Confocal microscope image of the microgel particle prepared from sample A2 (Table 1). Scale bar is 20 μm. (c) Gaussian fit to the size distribution of microgels prepared from sample A1 (Table 1) and transferred to the PBS buffer.

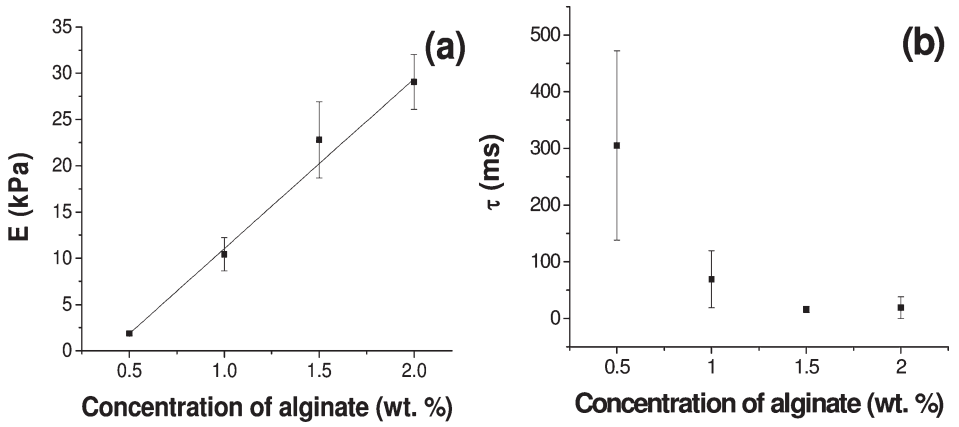

Figure 5. Variation in Young's modulus (a) and relaxation time (b) of the microgels plotted as a function of the concentration of sodium alginate in the droplet phase. All samples contained 4.0 wt % NIPAm and 10.0 wt % BIS (vs NIPAm) in the feed solution.

ratio is shown in Figure 4 and Table 2. As expected, the swelling of the hydrogels immersed in the buffer solution increased with decreasing concentration of alginate, NIPAm, and the degree of cross-linking in the samples. As the system contained more alginate or PNIPAm, it became more entangled and was swollen less by the buffer solution. The increase in the degree of cross-linking of PNIPAm tightened the hydrogel matrix and caused a decrease in the swelling of the sample as well.

Next, we characterized the mechanical properties of the microgels. We note that the use of the tipless cantilever could lead to uncertainty in its alignment with respect to the microgel particle; however, for each microgel series, the deviation in Young's modulus did not exceed 19%, suggesting that the effect of misalignment was insignificant. In addition, the use of a cantilever with similar dimensions to the microgels allows for indentation tests without pocking into the microgels, and the large cantilever should serve as a better probe for measuring the mechanical properties of the microgel as a whole, as opposed to a conical tip that probes locally on the surface in about hundreds of square nanometers.

For the microgels of series C, with increasing concentration of alginate, the Young's modulus increased from 1.86 to 29.0 kPa, that is, the microgels became stiffer (Figure 5a). The relaxation time of the microgels of series C was examined in stress relaxation experiments (as shown in Figure 1). With increasing concentration of alginate, the characteristic relaxation time of the microgels was reduced from 305 to 16 ms (Figure 5b). With introduction of alginate to the system, the network became more entangled and relaxed faster through the "thirion relaxation" mechanism.[35] The lower limit of the concentration of alginate yielded particles with Young's modulus values of 1.86 ± 0.23 kPa, which is within the range reported in the scientific literature for neutrophils.[4−6] In addition, the broad range of the variation of Young's modulus achieved by incremental variations in alginate concentration is within the Young's modulus of living cells (up to 100 kPa[36]).

Table 2 shows the Young's modulus and the relaxation time for the microgels with varying concentrations of NIPAm and BIS. Comparison of the properties of samples A1 and A2 showed a weak effect of the concentration of PNIPAm on the values of Young's modulus, E, and relaxation time, τ. Similarly, the values of E for the samples B1 and B2 were relatively close. To ascertain the polymerization of PNIPAm in the mixture with alginate, we conducted control experiments. PNIPAm microgels were prepared using the recipe of sample C4 (Table 1) but in the absence Ca^{2+} ions. Following the transfer of the microgels in the aqueous medium, they preserved their integrity owing to the polymerization of NIPAm. We ascribe the weak dependence of the mechanical properties of microgels on the concentration and degree of cross-linking of PNIPAm to the partition of NIPAm between the droplet and continuous phases in the MF reactor. Nevertheless, despite reduced concentration of PNIPAm in the microgels, it could be used for fine-tuning of the mechanical properties of the microgels.

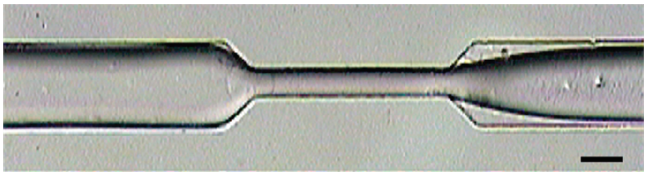

Figure 6. Snapshot of a microgel (sample C3) moving from a microchannel at large with a diameter of 180 μm to the constriction with a diameter of 50 μm. The microgel slows down and deforms at the entrance of the constriction. Scale bar is 100 μm.

In all samples, the stretching exponent varied from 0.4 to 0.6. The weak power law dependence was in agreement with the trends observed for other biological systems such as hepatoma cells and fibroblast cells,[31,37] suggesting that the IPN microgels show a cell-like behavior.

The application of the microgels as a model system for studies of flow of cells in blood capillaries was examined in microfluidics experiments. The microgel particles (series C) were introduced in a MF channel with a constriction. The microchannel was fabricated in poly(dimethylsiloxane) using a soft lithography method,[33] and its rectangular cross section was modified to make it circular.[38] The diameters of the channel at large and the constriction were 180 and 50 μm, respectively, thereby leading to substantial deformation of 100 μm diameter microgels. The flow of the microgels in the microchannel was recorded using a video recorder (Sony, GV-HD700). A snapshot picture of a typical flow experiment of sample C3 (Table 1) is shown in Figure 6. The microgels leave the channel at large and stop at the entrance to the constriction where they deform, in order to fit into the orifice (see the movie in the Supporting Information). After deformation, the microgels accelerated, moved through the orifice, and entered the channel at large.

Conclusions

We report a MF approach to the synthesis of IPN microgels with a narrow size distribution. The IPN microgels were characterized in light of the effect of each component of the microgels on their Young's modulus and relaxation time. We found that in the proposed approach the concentration of PNIPAm in the microgels and its degree of cross-linking did not have a significant effect on the mechanical properties of microgels, whereas the variation in alginate concentration had

a profound effect on the Young's modulus and relaxation time of the particles. The microgels became stiffer and relaxed faster when alginate content was increased. Our work has implications in two fields. First, a method to measure the macroscopic mechanical properties in the microscopic scale was developed. The Young's modulus and the relaxation time of the microgels were studied in AFM using a tipless cantilever, which allowed for an indentation tests without puncturing the microgels. Second, some of the IPN microgels described here have mechanical properties that are similar to living cells, in general, and to neutrophils, in particular. Therefore, these IPN microgels can be used as a model system in studies of flow of cells in constrained geometries.

Supporting Information Available: Images of PNIPAm microgels and a movie of the flow of a microgel particle in a microchannel (the video speed was reduced 10 times of its real time). This material is available free of charge via the Internet at http://pubs.acs.org.

References and Notes

(1) Huang, Y.; Doerschuk, C. M.; Kamm, R. D. *J. Appl. Physiol.* **2001**, *90*, 545–564.
(2) Sung, K. L. P.; Dong, C.; Schmid-Schonbein, G. W.; Chien, S.; Skalak, R. *Biophys. J.* **1988**, *54*, 331–336.
(3) Rezkalla, S. H.; Kloner, R. A. *Circulation* **2002**, *105*, 656–662.
(4) Roca-Cusachs, P.; Almendros, I.; Sunyer, R.; Gavara, N.; Farre, R.; Navajas, D. *Biophys. J.* **2006**, *91*, 3508–3518.
(5) Pleskova, S. N.; Gushchina, Y. Y.; Zvonkova, M. B.; Khomutov, A. E. *Bull. Exp. Biol. Med.* **2006**, *141*, 760–762.
(6) Wojcikiewicz, E. P.; Zhang, X. H.; Chen, A.; Moy, V. T. *J. Cell Sci.* **2003**, *116*, 2531–2539.
(7) Storka, K. M.; Aranda-Espiniza, H. *Cell Motil. Cytoskeleton* **2009**, *66*, 328–341.
(8) Xu, G.; Shao., J. Y. *Am. J. Physiol.: Cell Physiol.* **2008**, *295*, C1434–C1444.
(9) Hochmuth, R. M. *J. Biomech. Eng.* **1993**, *115*, 515–519.
(10) Schmid-Schonbein, G. W.; Sung, K. L. P.; Tozeren, H.; Skalak, R.; Chien, S. *Biophys. J.* **1981**, *36*, 243–256.
(11) Trans-Son-Tay, R.; Needham, D.; Yeung, A.; Hochmuth, R. M. *Biophys. J.* **1991**, *60*, 856–866.
(12) Bathe, M.; Shirai, A.; Doerschuk, C. M.; Kamm, R. D. *Biophys. J.* **2002**, *83*, 1917–1933.
(13) Yanai, M.; Butler, J. P.; Suzuki, T.; Sasaki, H.; Higuchi, H. *Am. J. Physiol. Cell Physiol.* **2004**, *287*, C603–C611.
(14) Brizard, A. M.; van Esch, J. H. *Soft Matter* **2009**, *5*, 1320–1327.
(15) Althoff, G.; Stauch, O.; Vilfan, M.; Frezzato, D.; Moro, G. J.; Hauser, P.; Schubert, R.; Kothe, G. *J. Phys. Chem. B* **2002**, *106*, 5517–5526.
(16) Cans, A. S.; Wittenberg, N.; Karlsson, R.; Sombers, L.; Karlsson, M.; Orwar, O.; Ewing, A. *Proc. Natl. Acad. Sci. U.S.A.* **2003**, *100*, 400–404.
(17) Fiddes, L. K.; Young, E. W. K.; Kumacheva, E.; Wheeler, A. R. *Lab Chip* **2007**, *7*, 863–867.
(18) Fiddes, L. K.; Chan, H. K. C.; Wyss, K.; Simmons, C. A.; Kumacheva, E.; Wheeler, A. R. *Lab Chip* **2009**, *9*, 286–290.
(19) Limozin, L.; Sackmann, E. *Phys. Rev. Lett.* **2002**, *89*, 1–4.
(20) Campillo, C. C.; Schroder, A. P.; Marques, C. M.; Pepin-Donat, B. *Mater. Sci. Eng., C* **2009**, *29*, 393–397.
(21) Nakayama, A.; Kakugo, A.; Gong, J. P.; Osada, Y.; Takai, M.; Erata, T.; Kawano, S. *Adv. Funct. Mater.* **2004**, *14*, 1124–1128.
(22) Gong, J. P.; Katsuyama, Y.; Kurokawa, T.; Osada, Y. *Adv. Mater.* **2003**, *15*, 1155–1158.
(23) Li, W.; Pham, H. H.; Nie, Z.; MacDonald, B.; Guenther, A.; Kumacheva, E. *J. Am. Chem. Soc.* **2008**, *130*, 9935–9941.
(24) Xu, S.; Nie, Z.; Seo, M.; Lewis, P.; Kumacheva, E.; Stone, H. A.; Garstecki, P.; Weibel, D. B.; Gitlin, G.; Whitesides, G. M. *Angew. Chem., Int. Ed.* **2005**, *44*, 724–728.
(25) Zhang, H.; Tumarkin, E.; Peerani, R.; Nie, Z.; Sullan, R. M. A.; Walker, G. C.; Kumacheva, E. *J. Am. Chem. Soc.* **2006**, *128*, 12205–12210.
(26) Zhang, H.; Tumarkin, E.; Sullan, R. M. A.; Walker, G. C.; Kumacheva, E. *Macromol. Rapid Commun.* **2007**, *28*, 527–538.
(27) Tumarkin, E.; Kumacheva, E. *Chem. Soc. Rev.* **2009**, *38*, 2161–2168.
(28) Hutter, J. L.; Bechhoefer, J. *Rev. Sci. Instrum.* **1993**, *64*, 1868–1873.
(29) Kocharova, N.; Lukkari, J.; Viinikanojal, A.; Aaritalo, T.; Kankare, J. *J. Mol. Struct.* **2003**, *651*, 75–83.
(30) Puttock, M. J.; Thaite, E. G. *Elastic Compression of Spheres and Cylinders at Point and Line Contact*; CSIRO: Melbourne, 1969; p 8.
(31) Okajima, T.; Tanaka, M.; Tsukiyama, S.; Kadowaki, T.; Yamamoto, S.; Shimomura, M.; Tokumoto, H. *Nanotechnology* **2007**, *18*, 1–5.
(32) Anna, S. L.; Bontoux, N.; Stone, H. A. *Appl. Phys. Lett.* **2003**, *82*, 364–366.
(33) Xia, Y.; Whitesides, G. M. *Angew. Chem., Int. Ed.* **1998**, *37*, 550–575.
(34) Kim, J. W.; Utada, A. S.; Fernandez-Nieves, A.; Hu, Z.; Weitz, D. A. *Angew. Chem., Int. Ed.* **2007**, *46*, 1819–1822.
(35) Sperling, L. H. *Introduction to Physical Polymer Science*, 3rd ed.; Wiley-Interscience: Hoboken, NJ, 2001; p 434.
(36) Radmacher, M. *IEEE Eng. Med. Biol.* **1997**, *16*, 47–57.
(37) Okajima, T.; Tanaka, M.; Tsukiyama, S.; Kadowaki, T.; Yamamoto, S.; Shimomura, M.; Tokumoto, H. *Jpn. J. Appl. Phys.* **2007**, *46*, 5552–5555.
(38) Fiddes, L. K.; Raz, N.; Srigunapalan, S.; Tumarkin, E.; Simmons, C. A.; Wheeler, A. R.; Kumacheva, E. *Biomaterials* **2010**, *31*, 3459–3464.